Hydro-geo-chemical streamflow analysis as a support for digital hydrograph filtering in a small, rainfall dominated, sandstone watershed

A. Longobardi*, P. Villani, D. Guida, A. Cuomo

Department of Civil Engineering, University of Salerno, 84084 Fisciano (SA), Italy

* Corresponding author. Via Giovanni Paolo II, 132, 84084 Fisciano (SA), Italy. Tel. +39 089 963408; e-mail address: alongobardi@unisa.it

"This is a post-peer-review, pre-copyedit version of an article published in Journal of Hydrology. The final authenticated version is available online at:http://dx.doi.org/10.1016/j.jhydrol.2016.05.028"

Abstract

The aim of the present study is an analysis of the ability of digital hydrograph filtering tools for the characterization of the baseflow source contributing to total streamflow for a typical, small, sandstone, rainfall dominated catchment. Daily streamflow and electrical conductivity data for an experimental catchment, the Ciciriello catchment, a 3km^2 watershed located in Southern Italy, have been collected to the purpose since 2012. The application of a mass balance filter (MBF), using electrical conductivity as tracer data, has pointed out a seasonal characterization of the baseflow pattern, contributing to total streamflow by 90% during the low flow period and up to 40% during the high flow period. The Lyne and Hollick one parameter and the two parameters Eckhardt digital filters have been furthermore processed, both in an uncalibrated and calibrated application. Providing a preliminary total streamflow and baseflow recession analysis, the one parameter filter appears particularly suited for ungauged cases, as the uncalibrated and calibrated applications are almost identical, with relative prediction errors, compared to MBF, smaller than 5%. The uncalibrated two parameters filter generates instead large relative error of about 35%. To improve the baseflow description, in particular during the low flow period, and to correct large (28%) underestimation of the minimum baseflow value, a seasonal calibration for the BFI_{max} parameter (the maximum BaseFlow Index that can be modelled by the filter algorithm) is in fact needed.

Keywords: hydrograph filtering, electrical conductivity, recursive digital filter, Mediterranean, Cilento UNESCO Global Geopark.

1. Introduction

The baseflow represents the slow streamflow component and it is generally related to groundwater outflows from shallow and deep aquifers, as in fact, regardless for the specific climate environment, its main features are tightly related to geological catchment properties (Mwakalila et al., 2002; Bloomfield et al., 2009; Mehaiguene et al., 2012; Longobardi and Villani, 2013; Ahiablame et al., 2013). Understanding the baseflow process is useful in many different water related issues, from water resources management strategies, low-flow conditions assessment, hydrological modelling calibration to water quality studies. Despite its importance, measurements of baseflow are actually unavailable, thus, hydrograph filtering approaches help to overcome this deficiency, providing a quantitative assessment of the slow streamflow component.

Hydrograph separation has been defined in the past as “one of the most desperate analysis techniques in use in hydrology” (Hewelett and Hibbert, 1967). In spite of a very broad number of experimental and analytical studies and of relevant scientific advances, the procedures available to this purpose are indeed still arbitrary, especially because the subjective influence of the user could impact the results (Rimmer and Hartmann, 2014). However, they provide a repeatable methodology to derive objective measures or indexes related to a particular streamflow source.

Several approaches are reported in the scientific literature for hydrograph filtering purposes. These can be grouped into analytical, empirical and mass balance methods (Stewart, 2015). Analytical methods are based on the fundamental theories of groundwater storage, often assuming ideal conditions that may not always be true (Boussinesq, 1877). Among others, empirical approaches have found considerable success: they are mainly based on a modelling framework, for which calibration is needed, based on field measurements or simply based on the user experience. Among these, a large number of recursive digital filters, assuming that the baseflow is the smooth frequency component of total hydrograph, have been proposed in the past literature (Lyne and Hollick, 1979; Nathan and McMahon, 1997; Chapman, 1999; Eckhardt, 2005; Aksoy et al., 2009). The mass balance methods are instead based on the assumption that baseflow has different chemical characteristics compared with surface runoff, because of the different residence times and flow paths of these two sources. Compared to others, the mass balance filtering method is considered to be an objective approach, because it is based on basin-specific physical processes and relevant monitoring activities. A wide use has been gained from the electrical conductivity used as

tracer for different water sources (Pinder and Jones, 1969; Lott and Stewart, 2013; Li et al., 2014; Longobardi et al., 2015). Electrical conductivity monitoring campaigns have been also successfully exploited for purpose of digital filter calibration (Stewart et al., 2007; Zang et al., 2013; Cartwright et al., 2014).

Even though able to separate a more realistic and plausible baseflow pattern, compared to more empirical methodologies, digital recursive filters still do not consider the hydrological phenomena behind the baseflow production and are disconnected from climate features which would however impact the baseflow generation (Furey and Gupta, 2001; Eckhardt, 2008; He et al., 2016; Lott and Stewart, 2016). In addition, the potential for their use has not yet been fully explored for particular hydro-geomorphological units, in particular for hard rock and rainfall-dominated catchments, for which there is a need to understand whether they are actually appropriate for such type of catchments (Eckhardt, 2005).

Focused on the relation between the geodiversity and ecosystem characteristics in the Cilento, Vallo Diano and Alburni National Park headwaters, a research program was launched in 2012. The program, currently granted by the UNESCO Cilento Global Geopark, promotes the monitoring activities performed in reference catchments, significant for the hydro-geodiversity of the sandstone landscapes, in the perspective of a progressive extension of the research tasks to similar catchments in other protected areas and Geoparks of the Mediterranean basin. Within this program, a 3km^2 drainage area, the Ciciriello catchment, has been instrumented to collect data to enhance the knowledge of the hydro-geomorphological behaviour of sandstone and forested units (Cuomo and Guida, 2013). Beyond traditional meteorological and streamflow measurements, geochemical properties have also been monitored, providing an objective approach to analyse the ability of digital hydrograph filtering tools for the characterization of the baseflow source contributing to total streamflow for small, rainfall dominated catchment, typical for sandstone landscapes. For the purpose, two different low-pass recursive digital algorithms have been selected, featured by and increasing level of flexibility and filter parameters. These are the Lyne and Hollick (1979) one parameter filter and the two parameters Eckhardt's filter (2005). The comparison with the mass balance approach will help addressing the selection of the most appropriate method for baseflow separation in case of poorly gauged catchments, for which tracer data are not available. An objective calibration of filter model parameters will furthermore address the ability of the

filters to adapt to markedly variable hydrological regimes resulting by markedly variable climate conditions.

2. The Ciciriello experimental catchment

2.1 The experimental watershed

The Ciciriello Watershed (LAT 40.1957 LONG 15.5379) is located in the southeast of Campania, Southern Italy. The area of the watershed is about 3km^2 and it is a dominantly forested area, without relevant human impacts. Elevation in the watershed ranges from 420 to 812 (M. Marchese) meters above mean sea level. The climate of the region is humid Mediterranean. Annual average precipitation is about 1400 mm with a marked difference between average maximum monthly summer precipitation, of about 30 mm, and average maximum monthly winter precipitation, of about 250 mm (Blasi et al., 2013).

From a hydro-geomorphological point-of-view, the Cilento and Vallo di Diano Geopark (Figure 1) consists of carbonate, sandstone and alluvial aquifers (Allocca et al., 2014). Sandstone aquifers, despite their great local interest in ecological issues, traditional agriculture and forestry maintenance, have had so far less attention than karst carbonate systems. Due to the lack of complete knowledge about the hydrological behavior of sandstone catchments within the Cilento and Vallo di Diano Geopark, the Ciciriello watershed has been chosen as an experimental catchment.

In the watershed, a southwestern dipping sandstone aquifer is resting in unconformity on a folded strata marly-clayey aquiclude. Along the western valley side, inter-bedded to the sandstone strata, a 10 m-thick lenticular marly bed outcrops (Figure 2). The bedrock is covered by thick regosols on the upper ridges, regolith on the noses and spurs and gravelly slope deposits at the toe of the open slopes. The stream bed is incised in alluvial, coarse deposits and partly on bedrock. Colluvium hollows are located in the bottom of the zero order basins. Permanent springs from bedrock aquifers and seasonal outflows from shallow, perched aquifers and colluvium deposits increase, progressively downstream, the stream discharge.

2.2 Data collection

Since December 2012, and currently in progress, a number of monitoring stations have been located along the drainage network of the Ciciriello watershed. The main station is located at the outlet of the catchment (420 m a.s.l.). In addition, secondary stations have been located just upstream from the main tributary junctions and downstream from the perennial bedrock springs and temporary seasonal through flow

outlets from the zero order basins (Figure 2). Location and timing of the monitoring activity have been based on detailed, multi-temporal hydro-geomorphological surveys and measurements, oriented by the "variable source areas" concept (Hewelett and Hibbert, 1967) and the "hydro-geomorphic paradigm" (Sidle et al., 2000).

Water depth (D), discharge (Q) and electrical conductivity (EC) have been measured, daily, at main station and, weekly, at the sub-stations. The Swoffer 3000 current meter (Swoffer Inc., USA) has been used for discharge measurements, and the HI9828 multi-parametric probe (Hanna Instruments Inc., Romania) for EC measurements. During selected storm events, 10-minute D and EC data have been moreover recorded at the main station by using the data logger DL/N70-Multi (STS Inc., Switzerland). Rainfall and temperature data, at 10-minute time resolution, for Sanza rain gauge have been provided by courtesy of the Civil Protection Service of the Campania Region.

3. Baseflow component characterization through mass balance approach

Monitored electrical conductivity data have been used for the application of a mass balance filter algorithm (MBF) to provide an objective description and characterization of the baseflow pattern and indices for the Ciciriello watershed. The objective MBF separation also enables highlighting similarities and differences in the hydrograph recession process for total and baseflow time series, useful for the following additional hydrograph separation applications.

3.1 Mass Balance Filtering (MBF)

The mass balance method is based on the assumption that baseflow has different chemical characteristics compared with surface runoff due to the different flow paths of these two types of flows. As a consequence, total streamflow hydrograph can be separated into different components on the base of the single component concentration. Mass balance, using the electrical conductivity EC as proxy of the Total dissolved solids (TDS), is one of the most widely used tracer technique. Total dissolved solids (TDS), in milligram/liter (ppm) and electrical conductivity (EC) in microSemiens/centimeter (μS/cm) are related by a conversion factor TDS/EC variable between 0.5-0.7, depending on which type of conversion is used, respectively, the NaCl conversion (sodium chloride) or the 442 conversion (40% sodium sulfate, 40% sodium bicarbonate, and 20% sodium chloride) (Atekwanaa et al (2004).

The baseflow component, in non-evaporitic terrains and unglaciated landscapes, has generally greater EC values compared to the surface runoff conductivity and, for this reason, EC can be used as a natural tracer of the streamflow component. This behaviour is particularly evident in the hydro-chemograph illustrated in Figure 3, where the measured EC approaches the largest values during the low flow period, corresponding to the period from early summer to late autumn in the humid Mediterranean climate, according to Cuomo and Guida (2016, under revision). It is possible to consider the following equations system (MBF):

$$\begin{cases} q_{tot}(t) = q_{sf}(t) + q_{bf}(t) \\ q_{tot}(t) \cdot EC_{tot}(t) = q_{sf}(t) \cdot EC_{sf}(t) + q_{bf}(t) \cdot EC_{bf}(t) \end{cases} \quad (1)$$

where

q_{tot} = measured total streamflow (l/s); q_{sf} = surface streamflow component (l/s); q_{bf} = baseflow streamflow component (l/s); EC_{tot}= measured streamflow EC (µS/cm); EC_{sf} = EC surface component (µS/cm) and EC_{bf} = EC baseflow component (µS/cm).

According to Stewart et al. (2007) and Li et al. (2014), an adequately long term monitoring activity ensures a full range of EC_{bf} and EC_{sf} variability to be explored. In this case EC_{bf} could be assumed as the end-member of the stream water conductivity during the period with the lowest streamflow, around 350 µS/cm, while EC_{sf} as the end-member of the stream water conductivity during the highest streamflow period, around 80 µS/cm. These values, according to Atekwanaa et al (2004), are considered proxy values of TDS values of 170 and 40 mg/l obtained from the Ciciriello catchment hydro-chemical data analysis. The consequent hydrograph separation is illustrated in Figure 3.

Considered as the ratio between the baseflow volume and the total streamflow volume, the Ciciriello watershed BaseFlow Index (BFI) is about 42%, consistent with the hydrogeological features of the catchment. Considering the climate characteristic of the studied area and the hydrogeological catchment properties, which emphasize the inter-annual hydrological response variability, it is important to note that both the total and baseflow discharge regimes are markedly seasonal (Figure 4). A low flow season exists, from June to November, when permanent bedrock springs sustain the streamflow and the baseflow component represents about 90% of total streamflow. A high flow period, from December to May, is counter posed, when baseflow represent only the 40% of total streamflow. In the following, it will be

showed that, accounting for this seasonal variability, is necessary to provide satisfactory performances in the application of particular recursive digital filters.

3.2 Recession analysis

The application of digital hydrograph filtering techniques requires, as in the following explanation, an analysis of the hydrograph recession process and an assessment of the recession constant, to be used as filter parameter.

The recession curve is the lower part of the falling limb of a hydrograph and expresses the relation between flow and time at low hydraulic heads. For purpose of hydrograph filtering, concern is pointed on the baseflow recession, as the streamflow recession during periods of no direct runoff (Chapman, 1999). Several curves have been suggested to represent the baseflow recession. The most used equation is the simple exponential relationship (Maillet, 1905):

$$Q_t = Q_0 e^{-\alpha t} = Q_0 k^t \quad (2)$$

where Q_t is the discharge at time t, Q_0 is the initial discharge and $k = e^{-\alpha t}$ is the recession constant and α is the recession rate. In particular environment, such as the karstic regions, the hydrograph recession limb can be furthermore featured by a decreasing or increasing recession rate during the depleting phase (Fiorillo, 2011).

A streamflow hydrograph recession analysis has been performed for about 30 events, where differences have been made between low flow and high flow periods. The analysed recession limbs (for the 30 events) have been extracted according to the following explanation. Hydrograph has been plotted on a semi-logarithmic scale and the recession curve has been identified when observed data where aligned along a straight line, assuming the linear reservoir concept would hold. During the recession phase two different segments are clearly identified, regardless for the seasons and the event. For clarification, an example, for two different low and high flow events, is illustrated in Figure 5. The largest recession rate (α_1) would represent the quicker drainage from the shallow aquifers, occurring after intense recharge during high water table conditions, whereas the smallest recession rate (α_2) would represent the slower draining from the deep aquifer occurring during low water table level condition, typically during the dry period (Fiorillo, 2011). The break between the two slopes is found by maximizing the goodness-of-fit for the total duration of the recession limb. For each of the components a minimum number of 4 days of observation has been considered to fit the linear reservoir equation. The α_2 is lower than α_1 regardless to

the event and to the season, with the lowest values for α_2 approached during the low flow season. Average value for the recession rates and recession constants are provided in Table 1 on a seasonal base. The rate α_2 would represent a reliable estimation of the recession rate of interest for baseflow separation.

The objective identification of the baseflow, provided by the mass balance equation using electrical conductivity data, allows the recession analysis to be performed for baseflow as well as for total flow, providing a more appropriate estimation for the baseflow recession constant. The baseflow recession process has been investigated for the same events selected for total streamflow recession analysis, and results have been illustrated both in Figure 5 and Table 1. As well as for total flow, two different segments are evident on the logarithmic plot, the slopes of which, although following the same rule ($\alpha_1 > \alpha_2$), are lower than total streamflow slopes. The most interesting consequence is the fact that very similar values have been found for α_2 for both total and baseflow recessions, regardless for the season. For the purpose of baseflow separation, this circumstance make reliable the use of the information derived from the observed total streamflow, with interesting consequences for ungauged catchments, where tracer data are not available.

Differences would have been significant for the case of an event scale analysis, where, compared to the daily scale herein analysed, more than two different mechanism of runoff production must be accounted for, as proposed in Cuomo and Guida (2016, under revision). In the following the comparison between an uncalibrated and a calibrated application of recursive digital filters will illustrates the practical implication.

4. Digital empirical hydrograph filtering

As previously mentioned, several approaches are reported in the scientific literature providing hydrograph filtering methods for baseflow identification purposes. Two different methods, belonging to the recursive digital filter group, have been applied for the Ciciriello experimental catchment data. These are the one parameter algorithm (Lyne and Hollick, 1979; Chapman, 1991; Chapman, 1999) and the Eckhardt's two parameters algorithm (Eckhardt, 2005). They have been applied as low-pass filters, providing the separation of the total streamflow signal, y, into the high frequency component f (runoff) and the low frequency component b (baseflow):

$$y_t = f_t + b_t \quad (3)$$

where t is the time index. Lyne and Hollick (1979) proposed the filter equation:

$$b_t = ab_{t-1} + \frac{1-a}{2}(y_t + y_{t-1}) \quad (4)$$

subject to the condition $b_t \leq y_t$, where a is the filter parameter. Chapman (1991) pointed out that the Lyne and Hollick algorithm incorrectly provides a constant baseflow b when direct runoff has ceased ($f = 0$), and therefore developed a new algorithm where the baseflow is a simple weighted average of the direct runoff and the baseflow at the previous time:

$$b_t = ab_{t-1} + (1-a)f_t \quad (5)$$

which can be transformed in the following equation:

$$b_t = \frac{a}{2-a}b_{t-1} + \frac{1-a}{2-a}y_t \quad (6)$$

when f is considered to be the difference between total and baseflow. Equation (6) is subject to the condition $b_t \leq y_t$, and a is the filter parameter that is the recession constant during period of no direct runoff (Chapman and Maxwell, 1996).

The Eckhardt filter algorithm has been demonstrated to be a flexible method and actually a number of one-parameter filters reported in the specific literature, are all special cases of the two-parameters Eckhardt's filter (Eckhardt, 2005). The baseflow component can be considered as:

$$b_t = Ab_{t-1} + By_t \quad (7)$$

subject to the restriction $b_t \leq y_t$. Assuming a linear relation between outflow from the aquifer and its storage, parameters A and B in Equation (7) can be expressed as functions of the recession constant a, and second parameter, called the BFI_{max}, the maximum BFI value the algorithm is able to model. The following expressions indeed hold:

$$\begin{cases} B = \dfrac{(1-a)\cdot BFI_{\max}}{1-a\cdot BFI_{\max}} \\ A = \left(\dfrac{1-BFI_{\max}}{1-a\cdot BFI_{\max}}\right)a \end{cases} \quad (8)$$

and the filter is then expressed as:

$$b_t = \frac{(1-BFI_{\max})ab_{t-1} + (1-a)BFI_{\max}y_t}{1-aBFI_{\max}} \quad (9)$$

subject to the restriction $b_t \leq y_t$. While the parameter a can be estimated by a recession analysis, there is no objective way to define BFI_{max}, for which the filter's author introduced pre-defined parameter

depending on geological and hydrogeological catchment properties. The author also suggested that these pre-defined values can cause tendentious approximations in the BFI calculation, and that the coupled use of different methods, such as tracer experiment, could be useful to optimize the parameter settings (Eckhardt, 2005).

5. Comparison between mass balance and digital filtering methods

Empirical approaches, and among these digital filters, have found considerable success and have gained a large popularity because of the possibility of application to many different hydro-geological and climate environments. They can be applied using pre-defined filter parameters but to achieve an adequate characterization of the baseflow component, a calibration phase is needed. The mentioned one parameter and two parameters filters have been applied for the Ciciriello catchment, both in uncalibrated and a calibrated procedures. For uncalibrated procedures, an application where filter parameters are set on pre-defined values (based on catchment properties) is intended. For calibrated procedures, an application where filter parameters, starting from pre-defined values, are tuned to reach a given result, is instead intended. MBF (baseflow separated through the application of the MBF filter) baseflow indices and statistics have been used for purpose of comparison and to proceed to the calibration phase. A statistical analysis is performed to compare uncalibrated and calibrated approaches.

5.1 Uncalibrated digital filters application

The application of the one parameter filter only requires the identification of the baseflow recession constant a (Eq. (6)). Results of the recession analysis previously reported have been used to this aim. If an uncalibrated application is under investigation, recession constant can of course only be assessed for total streamflow data. Table 1 results indicate that, at least for the studied catchment, the recession constant exhibits a seasonal variability (on average 0.96 during the low flow season and 0.86 during the high flow season). The recession analysis performed for the MBF baseflow series indicates that the same is not for the baseflow recession constant (on average 0.94 during the low flow season and 0.91 during the high flow season). The baseflow recession analysis further indicates that, on average, the total streamflow and the baseflow recession constant during the low flow season are comparable (respectively 0.96 and 0.94). In summary, for uncalibrated application to seasonal hydro-climate regimes catchments, the one parameter filter a could then be realistically assumed as the total streamflow recession constant during the

low flow period. For the Ciciriello watershed, a (= α_2) has been set to 0.96. This last value is also comparable to the upper extreme of the range of values (0.90-0.95) proposed by Nathan and McMahon (1990).

On the operational procedure, the one parameter filter has to be applied in a recursive algorithm. Rather frequently, the filter is used with three passes over the data (forward, backward and forward again), to smooth the baseflow series and to minimize the distortion effected produced by the filter itself (Nathan and McMahon, 1990; Li et al., 2014). Spongberg (2000) suggested that large values for the filter parameter have to be compensated by a small number of passes, as the high frequency is completely attenuated at the first step and further steps would only smooth the baseflow. Spongberg (2000) also suggested that an even number of passes would minimize the signal phase distortion. According to such indications and provided the large value (0.96) for the filter parameter, a number of two passes has been used for the case study.

The application of the two parameters filter requires an assessment for the parameter a, the recession constant, and for BFI_{max}. For the recession constant a, the discussion provided for the application of the one parameter filter will hold. Thus also in this case it is assumed a = α_2. For the BFI_{max}, a pre-defined parameter, depending on geological and hydrogeological catchment properties, can be set. The Ciciriello watershed belongs to the class of perennial streams with hard rock aquifers, for which pre-defined BFI_{max} is equal to 0.25.

Baseflow index and baseflow statistics are illustrated in Table 2 along with the percentage errors computed with reference to the MBF baseflow statistics. Results are also illustrated in Figure 6 (left panel) in terms of flow duration curves.

5.2 Digital filters calibration

Despite the very good performances, a calibrated version of the one parameter filter has been also provided. The calibration has been obtained comparing the results of the MBF separation with the digital filter application, minimizing the baseflow statistic percentage errors. The results of the calibration is a = 0.957, very similar to the parameter used in the uncalibrated application (0.96). Baseflow statistics and percentage errors are reported respectively in Table 3 and Table 4.

In order to calibrate the two parameters algorithm, provided the stability of the recession constant as illustrated in the calibration of the one parameter filter but also for purpose of application to ungauged

catchments where tracer data are not available, focus has been only set on the BFI_{max} parameter. Also in this case, the calibration has been obtained comparing the results of the MBF separation with the digital filter application, minimizing the baseflow statistic percentage errors. Assigned a = 0.96, the result of the calibration is a BFI_{max} = 0.47, which is rather different compared to the uncalibrated case (BFI_{max} = 0.25). Scientific statements about the error associated to an incorrect choice for the BFI_{max} value are indeed so far contradictory, as in many studies confirmation or rejection of the pre-defined BFI_{max} have been reported, without an evident and reliable explanation (Gonzales et al., 2009; Collishonn et al., 2013; Cartwright et al., 2014; Stewart, 2015). Baseflow statistics and percentage errors are reported respectively in Table 3 and Table 4.

EC data are undoubtedly valuable for the optimization of the parameter settings and minimization of prediction errors but they can be further exploited to set a calibration procedure that is best suited to the characteristics of the hydrological system under investigation.

The Ciciriello experimental catchment is a rainfall dominated hydrological system, for which distinct low and high flow periods can be identified within the hydrological regime. Seasonality is embedded in the climate and hydrological regime, but it is also hidden in the runoff generation, as indicated by the EC measurements. Figure 7 (left side) illustrates the average daily observed electrical conductivity pattern for a year-long time window. The blue dots indicate the observed EC for each of the Day Of the Year (DOY) and the constant red line represent their average value. It is evident how for about one half of the year (DOY 0 – 150) the EC is highly variable and below the average value, whereas for the second half (DOY 150 – 300), corresponding to the low flow period, it is rather stationary and consistently above the average value. Assuming the EC as a proxy of the water sources contributing to runoff, it appears that they are significantly different during the year, that in different seasons the system hydrological response is different and that such differences need to be accounted for in a conceptual descriptive scheme.

The MBF technique intrinsically represent such seasonal variability as the actual baseflow value at a particular day is constrained by the EC observed value at that day. Contrarily, the digital filters technique assumes the hydrological system to behave similarly for each period of the year as the filter parameters are unequivocally defined for the full time series. Evidently, the latter assumption poses a problem in the descriptive capability of a strongly seasonal system, where the runoff generation mechanism switch from one period to another.

To overcome the limit of the two parameters filter approach, a seasonal calibration of the same has been proposed. The optimization has been focused, also in this case, on the assessment of the optimal BFI_{max} value. Supported by the empirical evidence illustrated in Figure 4 that hold for the Ciciriello catchments, only two seasons, a low flow and an high flow season, have been considered and for each of them a BFI_{max} has been calibrated. Values for the recession parameters a are taken from the results of the total streamflow recession analysis (Table 2).

The patterns illustrated in Figure 7 (left side) delineate the period of the year when runoff production switches from one to another dominant water generation sources. June to November appears to be the season where runoff is almost entirely produced by groundwater resources and for which it has been found an optimal value of $BFI_{max,low}$ = 0.77 (a_{low} = 0.96). December to May is instead the season of the year dominated by the rainfall contribution to total discharge and for which it has been found an optimal value of $BFI_{max,high}$ = 0.38 (a_{high} = 0.86). Results have been illustrated in Table 3 and Table 4, as statistics assessments and percentage of relative errors, and in Figure 7 (right side) as flow duration curves.

5.3 Statistical analysis

In terms of uncalibrated procedures, it is clearly evident that the one parameter filter outperforms the more flexible two parameters algorithm. Percentage errors for global BFI index are about 2% for the first case and about 35% for the second case. The average baseflow process is also well described by the one parameter filter. Largest errors are detected for the maximum baseflow value, but this condition is common to both procedures. Flow duration curves are compared by the AAPE index estimated (for each of the applied methods) as in the following (Longobardi and Villani, 2013):

$$AAPE = \frac{1}{n}\sum_{i=1}^{n}\left|\frac{Q_{MBF,i} - Q_{FIL,i}}{Q_{MBF,i}}\right| \quad (10)$$

where i is the decile order, Q_{MBF},i is the MBF baseflow value corresponding to the i-th decile, Q_{FIL},i is the baseflow resulted from the different filter algorithms value corresponding to the i-th decile, n the considered deciles.

Compared to the MBF baseflow, the uncalibrated one parameter baseflow duration curve also presents almost an optimal fitting with an average AAPE of 20% (Table 5). The uncalibrated two parameters baseflow duration curve describes instead a significant underestimation of the baseflow for almost all of the durations with an average error of about 40% (Table 5).

With reference to the calibrated procedures, statistical performances for the calibrated one parameter filter are almost identical to the uncalibrated case. An improvement, compared to the uncalibrated case, is instead evident for the two parameters filter (Table 2 and Table 4) but large errors of about 28% are still found in the (under) prediction of baseflow minimum value. The maximum value is also over predicted, such as in the case of the one parameter filter, of about 12%. The AAPE index also results in an improvement moving from 40% to 19% (Figure 7 and Table 5). The seasonal calibration further improves the performance of the baseflow separation filter, especially for what concerns the underestimation of minimum baseflow values, which moves form about 28% for the traditional calibration to about 9%. The AAPE index results in a further improvement moving from 49% to 16% (Figure 7 and Table 5).

Beyond the comparison between main descriptive statistics, the empirical baseflow distribution for the MBF and the different applied filters are compared. The box plot in Figure 8 and the quantile-quantile plots in Figure 9 illustrates some of the distribution properties. In agreement with the MBF baseflow distribution, all of the analysed filters, both uncalibrated and calibrated, generate asymmetric distributions, for which the larger discrepancies occur for the larger order percentiles assessment, maximum values and outliers consistency. Besides the main descriptive statistics already introduced, the one parameter filter for the uncalibrated and calibrated cases distributions are also equivalent and very close to the MBF distribution until the 90% percentile. Indeed the AAPE index is about 10%, half of the index value corresponding to the 100% percentile (Table 5 and Figure 9). The calibration and more evidently the seasonal calibration for the two parameters filter also results in an improvement in the empirical distribution compared to the MBF. The calibrated two parameters filter distribution adapts to the MBF distribution with an AAPE error of about 10% until the 80% percentile (Table 5 and Figure 9) but significantly differs for lager percentiles order (AAPE = 19% for 100% percentile). The seasonal calibrated two parameters filter represents the outperforming method: the outlier consistency is similar to the MBF distribution and, as the one parameter filter, it adapts the MBF distribution until the 90% percentile with smaller errors for larger percentile orders (Table 5 and Figure 9).

6. Discussion and conclusion

The paper has presented an analysis of the ability of digital hydrograph filtering tools for the characterization of the baseflow source contributing to total streamflow for a typical, small, sandstone,

419 rainfall-dominated catchment. Electrical conductivity monitoring data and the related objective mass
420 balance hydrograph separation, have provided useful indication about the selection, application and
421 calibration for digital filters for seasonal flow regimes and have moreover provided, for these particular
422 cases, practical indication for baseflow separation for catchments where tracer data are not available.

423 One of the main result deals indeed with the one parameter filter, only based on the assessment of the
424 recession constant, which appear to be the most efficient in the description of the baseflow pattern and
425 empirical distribution. The larger flexibility, embedded at least within the conceptual description by the
426 two parameters filter, appears instead as a complexity for a strongly seasonal hydrological system, such as
427 the studied catchment. It would indeed require a larger number of parameters to be calibrated, two for
428 each of the identified seasons, in order to get reliable baseflow pattern description and empirical
429 distribution, especially for what concerns the low flow season assessment.

430 Concerning the application of baseflow digital filtering techniques to watersheds where tracer data are not
431 available, and at least for the class of catchments to which the investigated system belongs, the presented
432 paper has pointed out the feasibility for a reliable recession constant to be derived by the total streamflow
433 analysis, performing an accurate calibration of recession events during the low flow season, which has
434 appeared to be the most critical for the investigated basin.

435 During the high flow period, the one and the two parameters filters are respectively associated to an
436 overestimation (20%) and underestimation (10%). For this period of the year, the monitoring campaign
437 strongly indicates a large range of variability for the EC values, probably caused by not only dilution and
438 mixing, but also by dispersion processes from different water sources and flow paths (Cuomo and Guida
439 2016, under revision). The variability is intrinsically embedded within the MBF method but it is not at all
440 accounted for by the digital filters, which are only able to distinguish between two different component
441 and between two main dominating runoff production mechanisms. The one parameter filter, basically
442 calibrated on the low flow season, in fact produces good estimates of the minimum value of baseflow (5%
443 error) while considerable overestimation (20%) is found for the highest values, typically occurring during
444 the high flow season. The two parameters filter, seasonally calibrated, produces errors comparable to the
445 one parameter filter for what concerns the minimum (10%) but it is able to enhance also the description of
446 the maximum values, with a reduction of the error (in underestimation) of 10%. The relative outlier

consistency is similar to the MBF distribution and it adapts the MBF distribution until the 90% percentile with smaller errors for larger percentile orders.

Digital filters, at least for the case study and for similar conditions, appear then sufficiently adequate to estimate time averages baseflow at annual scale from daily streamflow data. At the same time, they are not suitable for a more realistic representation of the baseflow pattern and its seasonal variability. More articulate conceptualization of the hydrological behaviour of the catchment, including different runoff generation mechanisms and a high-frequency data recording would be needed for an improvement, taking groundwater ridging, excess saturation and soil pipe runoff into account (Longobardi et al. 2014; Cuomo and Guida 2016, under revision).

Acknowledgments

The authors gratefully acknowledge funding support provided through the Instruction, University and Research Italian Ministry (MIUR) under the grant ORSA149974 and ORSA154528 and CUGRI. Thanks to Angelo De Vita and Aniello Aloia, respectively director and manager of the Cilento UNESCO Global Geopark for financial and logistic support in the research and Pasqualino Lovisi for the field collaboration and measurements. The authors thank the reviewers and the associate editor Steve Worthington, who handled this manuscript, for their helpful comments and encouragements, which resulted in a significant improvement of the manuscript.

References

Ahiablame, L., Chaubey, I., Engel, B., Cherkauer, K., Merwadec, V., 2013. Estimation of annual baseflow at ungauged sites in Indiana USA. J. Hydrol., 476, 13-27.

Aksoy, H., Kurt, I., Eris, E., 2009. Filtered smoothed minima baseflow separation method. J. Hydrol., 372 (1-4), 94-101.

Allocca, V., Manna, F., De Vita, P., 2014. Estimating annual groundwater recharge coefficient for karst aquifers of the southern Apennines (Italy). Hydrol. Earth Syst. Sc., 18, 803–817.

Aloia A., Calcaterra D., De Vita A., Guida D. (eds), 2013. Water and earth: resources and natural hazards. Geopark's Book n. 2 National Park of Cilento, Vallo di Diano e Alburni. 80 p.p.

Atekwanaa, E.A., Atekwanaa, E.A.; Rowe, R.S., Dale Werkema, D., Legalld, F.D., 2004. The relationship of total dissolved solids measurements to bulk electrical conductivity in an aquifer contaminated with hydrocarbon. Journal of Applied Geophysics, 56 (4): 281–294.

Smiraglia, D., Capotorti, G., Guida, D., Mollo, B., Siervo, V., Blasi, C., 2013. Land units map of Italy. Journal of Maps, 9 (2), 239-244.

Bloomfield, J.P., Allen, D.J., Griffiths, K.J., 2009. Examining geological controls on baseflow index (BFI) using regression analysis: An illustration from the Thames Basin, UK. J. Hydrol., 373 (1-2), 164-176.

Boussinesq J., 1877. Essai sur la théorie des eaux courantes. Memoires de l'Academie des Sciences de l'Institut de France, 23, 252–260.

Cartwright, I., Gilfedder, B., Hofmann, H., 2014. Contrasts between estimates of baseflow help discern multiple sources of water contributing to rivers. Hydrol. Earth Syst. Sc., 18 (1), 5-30.

Chapman, T. G., 1991. `Comment on ``Evaluation of automated techniques for baseflow and recession analyses'', by Nathan, R. J. and McMahon', T. A. (eds), Wat. Resour. Res., 27, 1783-1784.

Chapman, T., 1999. A comparison of algorithms for streamflow recession and baseflow separation. Hydrol. Process., 13, 701-714.

Chapman, T. G., Maxwell, A.I., 1996. `Baseflow separation - comparison of numerical methods with tracer experiments'. Hydrol. and Water Resour. Symp., Institution of Engineers, Australia, Hobart, 539-545.

Collischonn, W., Mainardi Fan, F., 2013. Defining parameters for Eckhardt's digital baseflow filter. Hydrol. Process., 27, 2614–2622.

Cuomo, A., Guida, D., 2013. Discharge-electrical conductivity relationship in the T. Ciciriello, a reference catchment of the Cilento, Vallo Diano and Alburni European Geopark (Southern Italy). Rend. Online Soc. Geol. It., 28, 36-40.

Cuomo, A., Guida, D., 2016. Using hydro-chemograph analises to reveal runoff generation processes in a Mediterranean catchment. Hydrol. Process., under review, Manuscript ID HYP-16-0037.

Eckhardt, K., 2005. How to construct recursive digital filters for baseflow separation. Hydrol. Process., 19, 507-515.

Eckhardt, K., 2008. A comparison of baseflow indices, which were calculated with seven different baseflow separation methods. J. Hydrol., 352 (1-2), 168-173.

Fiorillo, F., 2011. Tank-reservoir drainage as a simulation of the recession limb of karst spring hydrographs. Hydrogeol. J., 19 (5), 1009-1019.

Furey, P.R., Gupta, V.K., 2001. A physically based filter for separating base flow from streamflow time series. Water Resour. Res, 37 (11), 2709-2722.

Gonzales, A.L., Nonner, J., Heijkers, J., Uhlenbrook, S., 2009. Comparison of different base flow separation methods in a lowland catchment. Hydrol. Earth Syst. Sc., 13 (11), 2055-2068.

He, S., Li, S., Xie, R., Lu, J., 2016. Baseflow separation based on a meteorology-corrected nonlinear reservoir algorithm in a typical rainy agricultural watershed. J. Hydrol., 535, 418-428.

Hewelett, J.D., Hibbert, A.R., 1967. Factors affecting the response of small watershed to precipitation in humid areas, in International Symposium of Forest hydrology, Pergammon press, 275-290.

Li, Q., Xing, Z., Danielescu, S., Li, S., Jiang, Y., Meng, F.-R., 2014. Data requirements for using combined conductivity mass balance and recursive digital filter method to estimate groundwater recharge in a small watershed, New Brunswick, Canada. J. Hydrol. , 511, 658-664.

Longobardi, A., Villani, P., 2013. A statistical parsimonious empirical framework for regional flow duration curve shape prediction in a large permeability Mediterranean region. J. Hydrol., 507, 174-185.

Longobardi, A., Guida, D., Cuomo, A., Villani, P., 2015. At which time step do we need to monitor the stream hydro-chemistry properties for low flow characterization? Rend. Online Soc. Geol. It., 35, 188-191.

Lott, D.A., Stewart, M.T., 2013. A Power Function Method for Estimating BaseFlow. Ground Water, 51, 442–451.

Lott, D.A., Stewart, M.T., 2016. Base flow separation: A comparison of analytical and mass balance methods. J. Hydrol., 535, 525-533.

Lyne, V.D., Hollick, M., 1979. Stochastic time-variable rainfall runoff modelling. Hydrology and Water Resources Symposium, Institution of Engineers, Australia, Perth, 89-92.

Maillet, E., 1905. Essais d'hydraulique souterrain et fluviale, Librairie Scientifique, A. Hermann, Paris, 218.

Mehaiguene, M., Meddi, M., Longobardi, A., Toumi, S., 2012. Low flows quantification and regionalization in North West Algeria. J. Arid Environ., 87, 67-76.

Mwakalila, S., Feyen, J., Wyseure, G., 2002. The influence of physical catchment properties on baseflow in semi-arid environments. J. Arid Environ., 52, 245–258.

Nathan, R.J., McMahon, T.A., 1990. Evaluation of automated techniques for baseflow and recession analyses. Water Resour. Res., 26 (7), 1465-1473.

Pinder, G.F., Jones, J.F., 1969. Determination of the ground-water component of peak discharge from the chemistry of total runoff. Water Resour. Res., 5, 438–445.

Rimmer, A., Hartmann, A., 2014. Optimal hydrograph separation filter to evaluate transport routines of hydrological models. J. Hydrol., 514, 249-257.

Sidle, R.C., Tsuboyama, Y., Noguchi, S., Hosoda, I., Fujieda, M. Shimizu, T., 2000. Stormflow generation in steep forested headwaters: a linked hydrogeomorphic paradigm. Hydrol. Process., 14, 369-385.

Spongberg, M.E., 2000. Spectral analysis of base flow separation with digital filters. Water Resour. Res., 36 (3), 745-752.

Stewart, M., Cimino, J., Ross, M., 2007. Calibration of Base Flow Separation Methods with Streamflow Conductivity, Ground Water, 45, 17–27.

Stewart, M. K., 2015. Promising new baseflow separation and recession analysis methods applied to streamflow at Glendhu Catchment, New Zealand. Hydrol. Earth Syst. Sci., 19, 2587–2603.

Zhang, R., Li, Q., Chow, T.L., Li, S., Danielescu, S., 2013. Baseflow separation in a small watershed in New Brunswick Canada, using a recursive digital filter calibrated with the conductivity mass balance method. Hydrol. Process. , 27, 2659–2665.

Figure captions

Figure 1: Hydrogeological scheme of the Cilento UNESCO Global Geopark (Aloia et al., 2013). The experimental studied catchment location is indicated by a yellow box in the south eastern area of the Cilento Global Geopark.

Figure 2: Schematic geological map and monitoring stations of the Ciciriello experimental catchment (Cilento UNESCO Global Geopark).

Figure 3: Discharge, MBF baseflow separation and electrical conductivity measurements at the T. Ciciriello watershed main station.

Figure 4: Figure 4. Mean monthly MBF baseflow contribution to total streamflow at T. Ciciriello watershed main station.

Figure 5: Recession analysis during low flow period (left panel) and high flow period (right panel).

Figure 6: Left side. Electrical conductivity mass balance filtering (MBF) and recursive digital filters (one and two parameters) baseflow duration curves. Right side. Calibrated two parameters filter baseflow underestimation during low flow period.

Figure 7. Left side. Electrical conductivity annual pattern. Right side. MBF, calibrated and seasonally calibrated two parameters baseflow duration curves.

Figure 8. Box plot for mass balance, uncalibrated and calibrated one and two parameters filters application.

Figure 9. Quantile-quantile plot for mass balance versus uncalibrated and calibrated one and two parameters filters application.

Table captions

Table 1: Seasonal assessment for the smallest component of the recession rate (α_2) and related recession constant (k_2) for both total and baseflow.

Table 2: Baseflow statistics for MBF, uncalibrated one and two parameters filters. Errors refer to MBF baseflow separation.

Table 3: Baseflow statistics for MBF, calibrated one and two parameters filters.

Table 4: Percentage errors (comparison with MBF baseflow) for calibrated one and two parameters filters.

Table 5. AAPE index (%) for uncalibrated and calibrated one and two parameters filters.

Table 1. Seasonal assessment for the smallest component of the recession rate (α_2) and related recession constant (k_2) for both total and baseflow.

	Low flow period		High flow period	
	α_2	k_2	α_2	k_2
totalflow	0.04	0.96	0.15	0.86
baseflow	0.06	0.94	0.16	0.91

Table 2. Baseflow statistics for MBF, uncalibrated one and two parameters filters. Errors refer to MBF baseflow separation

	MBF	One parameter (a = 0.96)	Two parameters (a = 0.96; BFI_{max} = 0.25)	One parameter (% error)	Two parameters (% error)
BFI	0.42	0.41	0.27	2.38	35.71
Min (l/s)	1.75	1.67	0.68	4.57	61.14
Mean (l/s)	34.25	33.70	22.13	1.61	35.39
Max (l/s)	262.01	200.06	111.81	23.64	57.33
Std (l/s)	45.18	44.90	25.47	0.62	43.63

Table 3. Baseflow statistics for MBF, calibrated one and two parameters filters.

	One parameter (a = 0.957)	Two parameters (a = 0.96; BFI_{max} = 0.47)	Two parameters (a_{low} = 0.96; $BFI_{max,low}$ = 0.77) (a_{high} = 0.86; $BFI_{max,high}$ = 0.38)
BFI	0.42	0.42	0.42
Min (l/s)	1.67	1.26	1.41
Mean (l/s)	34.22	34.60	34.32
Max (l/s)	207.86	230.17	290.13
Std (l/s)	45.95	45.98	49.09

Table 4. Percentage errors (comparison with MBF baseflow) for calibrated one and two parameters filters.

	One parameter (a = 0.957)	Two parameters (a = 0.96; BFI_{max} = 0.47)	Two parameters (a_{low} = 0.96; $BFI_{max,low}$ = 0.77) (a_{high} = 0.86; $BFI_{max,high}$ = 0.38)
BFI	0.00	0.00	0.00
Min (l/s)	4.57	28.00	9.20
Mean (l/s)	0.09	-1.02	-0.20
Max (l/s)	20.67	12.15	-10.73
Std (l/s)	-1.70	-1.77	-8.65

Table 5. AAPE index (%) for uncalibrated and calibrated one and two parameters filters.

decile	One param. uncalibrated	Two param. uncalibrated	One param. calibrated	Two param. calibrated	Two seasonal calibrated
80%	9	28	10	12	12
90%	10	34	10	16	14
100%	19	40	19	19	16

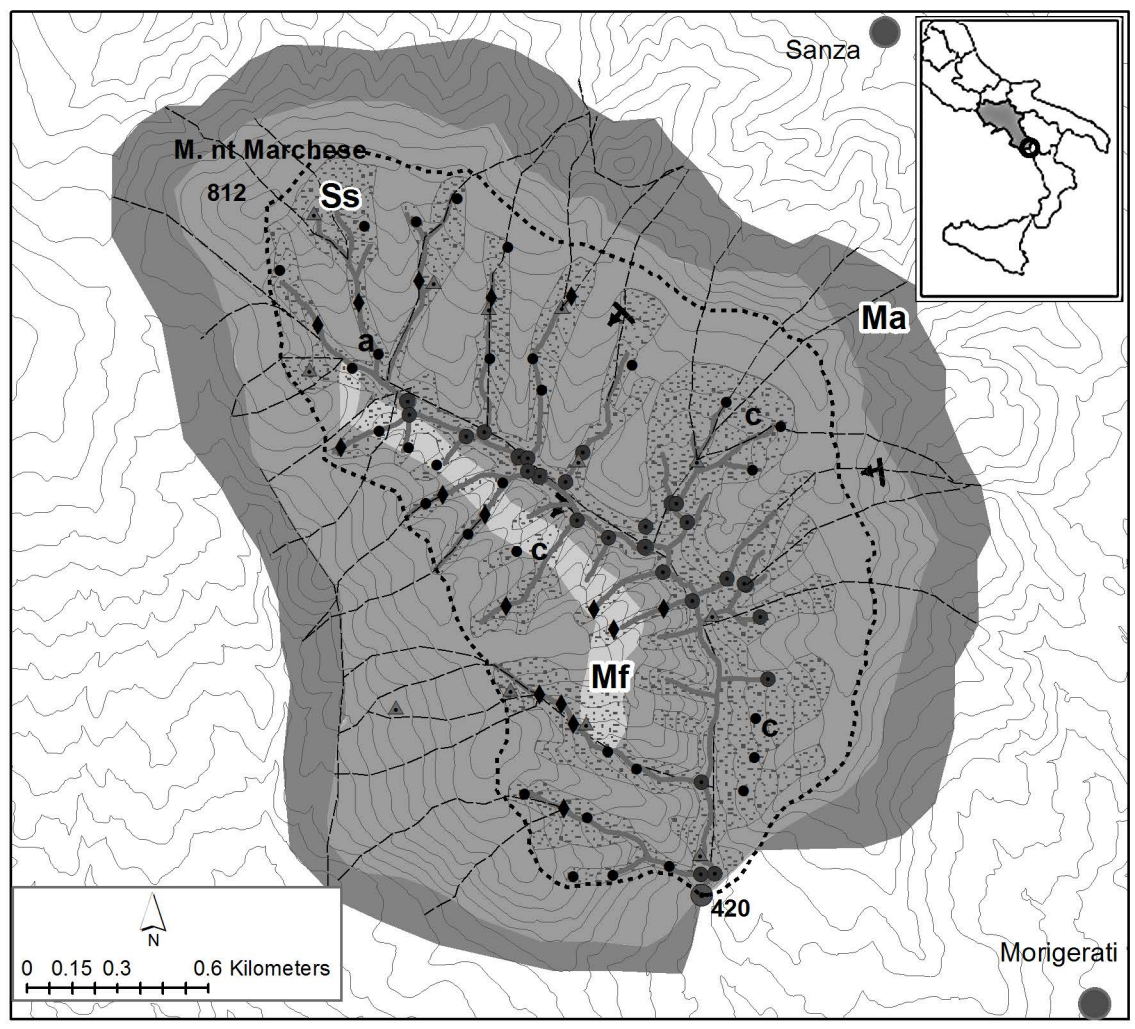

Bedrock

- Mf — Marly
- Ss — Sandstone
- Ma — Marly-clayey
- ---- Fault
- Strata attitude

Soil

- c — Colluvial
- a — Alluvial

Monitoring system

- Main station
- Sub station
- Secondary station
- Zob_riparian corridor station (weir/ piezometer)
- Spring station
- Rain gauge
- Control point

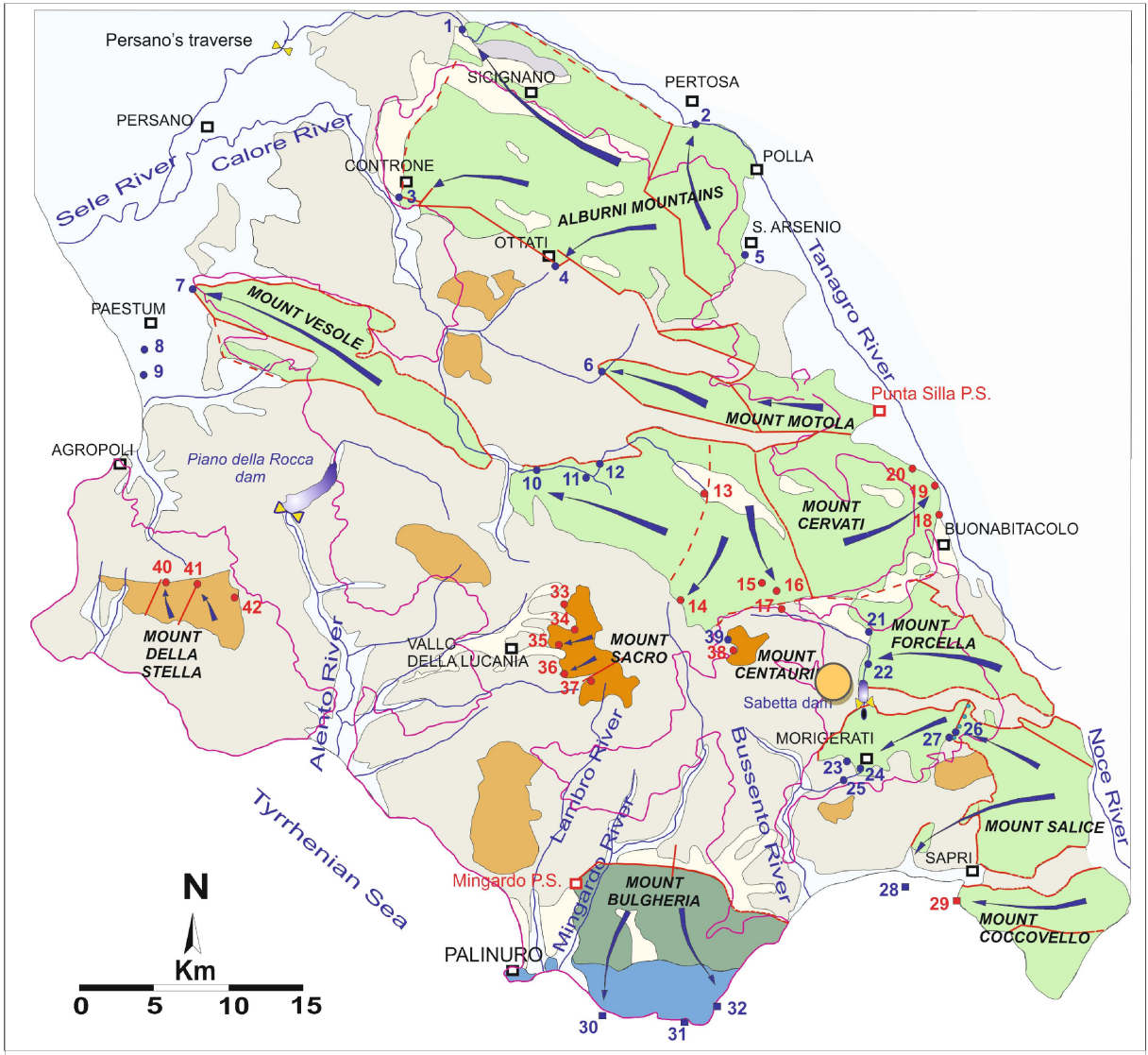

Legend

- Alluvial complex
- Detrital complex
- Conglomeratic-arenaceous complex (medium grade of permeability)
- Arenaceous-conglomeratic complex (medium-low grade of permeability)
- Pelitic-arenaceous-calcareous complex (low grade of permeability)
- Carbonate complex (high grade of permeability)
- Carbonate-detrital complex (high-medium grade of permeability)
- Carbonate-dolomitic complex (medium grade of permeability)
- Ciciriello Study area
- Boundary of the Cilento and Diano Valley Geopark
- Main tectonic features of hydrogeological relevance
- Principal subaerial springs, untapped and tapped respectively
- Submarine springs, untapped and tapped respectively
- Principal pumping-well stations
- Directions of groundwater flow
- Karst sinkhole
- Dams (Piano della Rocca e Sabetta)
- Principal hydraulic works of derivation and weir

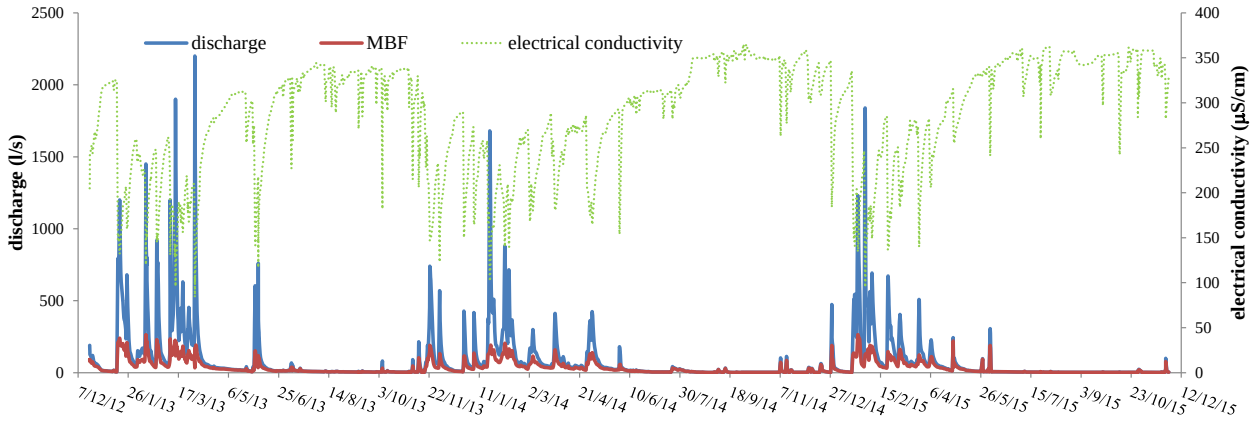

Figure 3. Discharge, MBF baseflow separation and electrical conductivity measurements at the T. Ciciriello watershed main station.

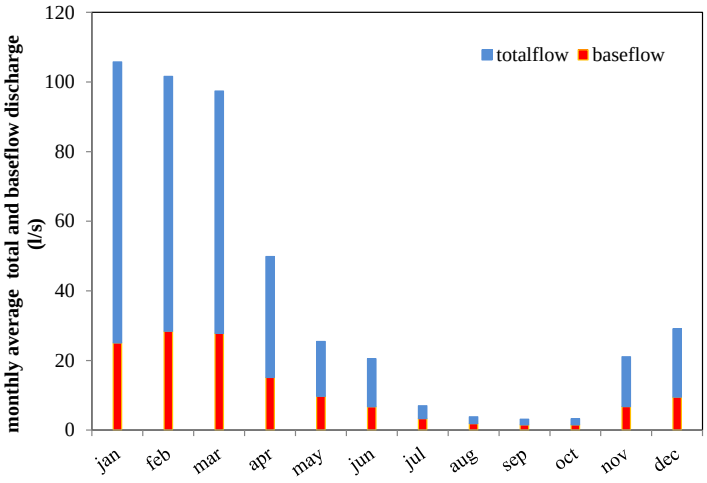

Figure 4. Mean monthly MBF baseflow contribution to total streamflow at T. Ciciriello watershed main station.

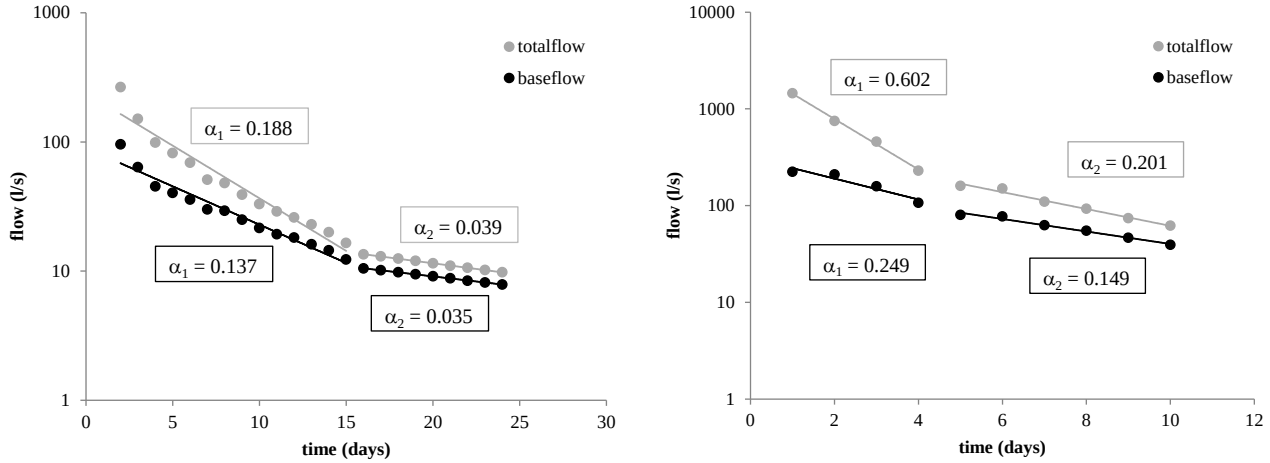

Figure 5. Recession analysis during low flow period (left panel) and high flow period (right panel).

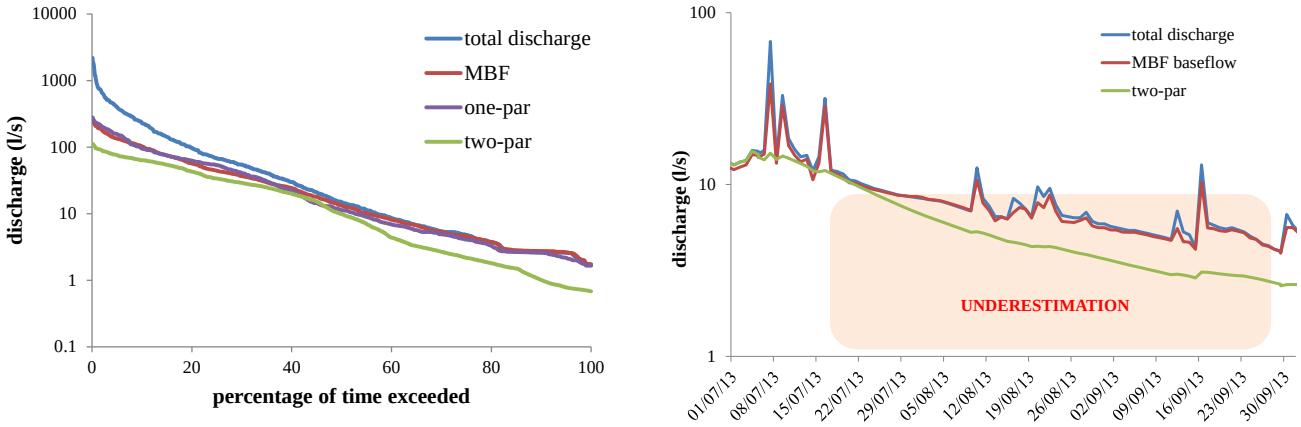

Figure 6. Left side. Baseflow duration curves for mass balance filtering (MBF), uncalibrated digital filters (one and two parameters). Right side. Calibrated two parameters filter baseflow underestimation during low flow period.

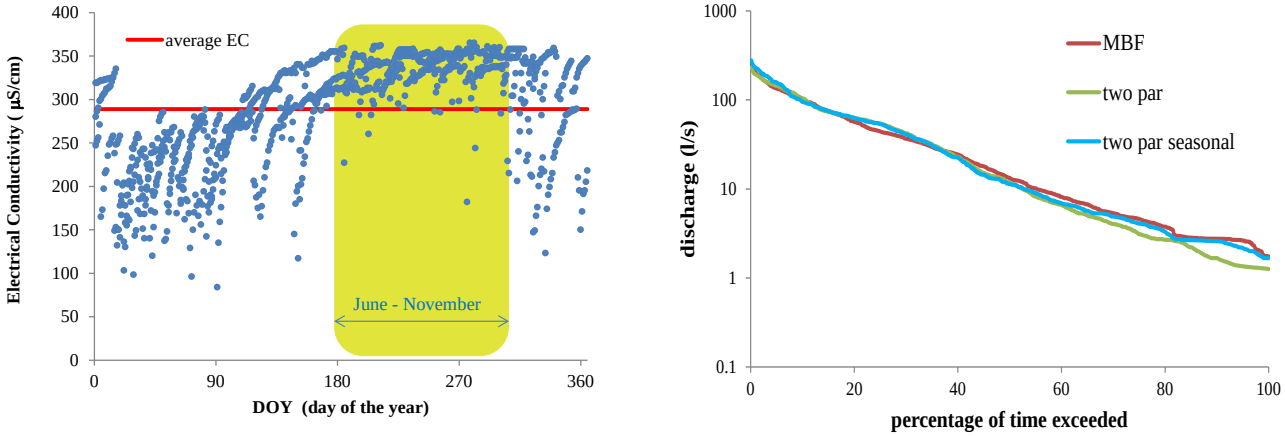

Figure 7. Left side. Electrical conductivity annual pattern. Right side. MBF, calibrated and seasonally calibrated two parameters baseflow duration curves.

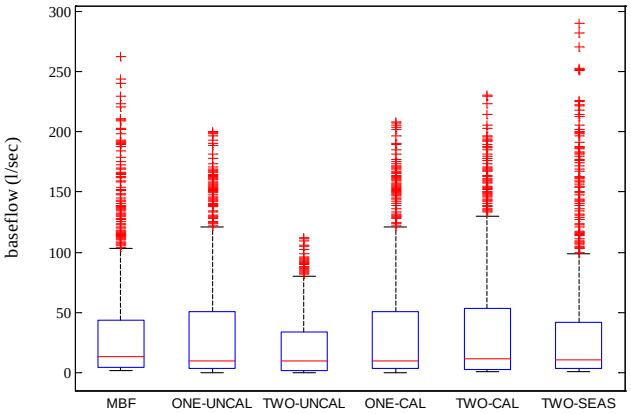

Figure 8. Box plot for mass balance, uncalibrated and calibrated one and two parameters filters application.

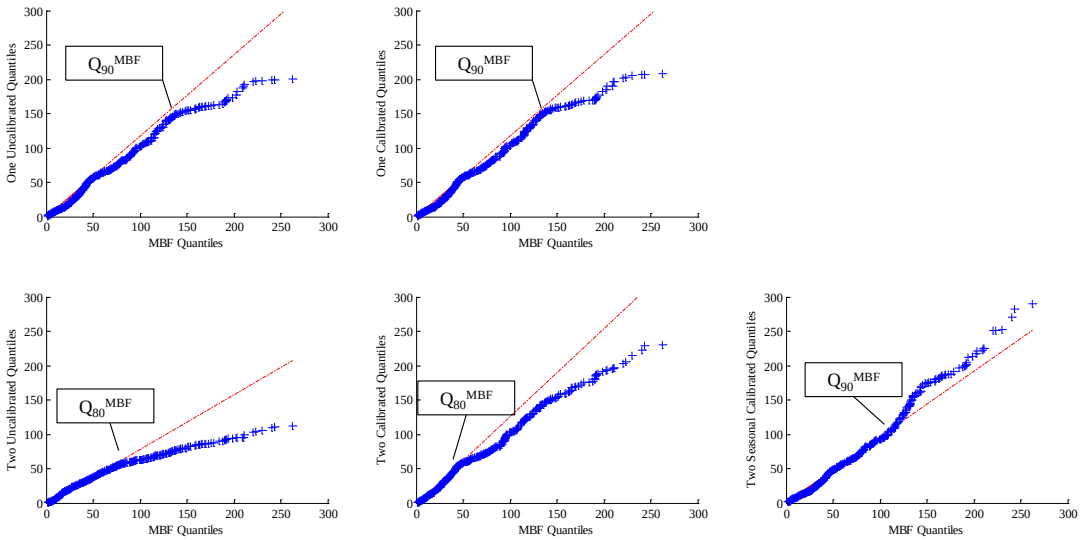

Figure 9. Quantile-quantile plot for mass balance versus uncalibrated and calibrated one and two parameters filters application.

Table 1. Seasonal assessment for the smallest component of the recession rate (α_2) and related recession constant (k_2) for both total and baseflow.

	Low flow period		High flow period	
	α_2	k_2	α_2	k_2
totalflow	0.04	0.96	0.15	0.86
baseflow	0.06	0.94	0.16	0.91

Table 2. Baseflow statistics for MBF, uncalibrated one and two parameters filters. Errors refer to MBF baseflow separation

	MBF	One parameter (a = 0.96)	Two parameters (a = 0.96; BFI_{max} = 0.25)	One parameter (% error)	Two parameters (% error)
BFI	0.42	0.41	0.27	2.38	35.71
Min (l/s)	1.75	1.67	0.68	4.57	61.14
Mean (l/s)	34.25	33.70	22.13	1.61	35.39
Max (l/s)	262.01	200.06	111.81	23.64	57.33
Std (l/s)	45.18	44.90	25.47	0.62	43.63

Table 3. Baseflow statistics for MBF, calibrated one and two parameters filters.

	One parameter (a = 0.957)	Two parameters (a = 0.96; BFI_{max} = 0.47)	Two parameters (a_{low} = 0.96; $BFI_{max,low}$ = 0.77) (a_{high} = 0.86; $BFI_{max,high}$ = 0.38)
BFI	0.42	0.42	0.42
Min (l/s)	1.67	1.26	1.41
Mean (l/s)	34.22	34.60	34.32
Max (l/s)	207.86	230.17	290.13
Std (l/s)	45.95	45.98	49.09

Table 4. Percentage errors (comparison with MBF baseflow) for calibrated one and two parameters filters.

	One parameter (a = 0.957)	Two parameters (a = 0.96; BFI_{max} = 0.47)	Two parameters (a_{low} = 0.96; $BFI_{max,low}$ = 0.77) (a_{high} = 0.86; $BFI_{max,high}$ = 0.38)
BFI	0.00	0.00	0.00
Min (l/s)	4.57	28.00	9.20
Mean (l/s)	0.09	-1.02	-0.20
Max (l/s)	20.67	12.15	-10.73
Std (l/s)	-1.70	-1.77	-8.65

Table 5. AAPE index (%) for uncalibrated and calibrated one and two parameters filters.

decile	One param. uncalibrated	Two param. uncalibrated	One param. calibrated	Two param. calibrated	Two seasonal calibrated
80%	9	28	10	12	12
90%	10	34	10	16	14
100%	19	40	19	19	16